

Imprinted [G-3]₈-T(3,5-OH)P(6)

To a solution of 102 mg (9.88 μmol) of **5** dissolved in 15 ml of THF, was added 10 ml of 2.5 M aqueous KOH. The reaction mixture was stirred vigorously at reflux until the reaction was complete by TLC. The reaction was stopped by removing the THF under reduced pressure. The resulting aqueous layer was extracted with CHCl₃ (3 × 25 ml). The combined organic layers were washed with 1 M aqueous HCl and water, and concentrated under reduced pressure. The product was dried under vacuum to afford 41.5 mg (43%) of **6** as a beige powder: ¹H NMR δ 7.23 (bs, 16H), 6.51 (bs, 152H), 5.86 (bs, ~4H), 5.60 (bs, ~60H), 5.12 (bs, ~8H), 4.86 (bs, 96H), 3.92 (bs, 128H), 2.45 (bs, 128H); MS (MALDI-TOF) *m/z* 9,710.8 (M + Na⁺ - 31C₂H₄ - C₄₄H₁₄N₄), 9,756.0 (M + K⁺ - 30C₂H₄ - C₄₄H₁₄N₄), 9,779.8 (M + K⁺ - 29C₂H₄ - C₄₄H₁₄N₄), 9,810.7 (M + K⁺ - 28C₂H₄ - C₄₄H₁₄N₄). Analysis: calculated for C₅₈₈H₆₀₀O₁₂₈: C, 72.70; H, 6.22; N, 0.00; Ru, 0.00. Found: C, 70.83; H, 6.19; N, 0.00; Ru, 0.00.

Received 28 February; accepted 28 May 2002; doi:10.1038/nature00877.

1. Wulff, G. & Sarhan, A. The use of polymers with enzyme-analogous structures for the resolution of racemates. *Angew. Chem. Int. Edn Engl.* **11**, 341–343 (1972).
2. Shea, K. J. Molecular imprinting of synthetic network polymers: the de novo synthesis of macromolecular binding and catalytic sites. *Trends Polym. Sci.* **2**, 166–173 (1994).
3. Andersson, L., Sellergren, B. & Mosbach, K. Imprinting of amino acid derivatives in macroporous polymers. *Tetrahedr. Lett.* **25**, 5211–5214 (1984).
4. Katz, A. & Davis, M. E. Molecular imprinting of bulk, microporous silica. *Nature* **403**, 286–289 (2000).
5. Wulff, G. Molecular imprinting in cross-linked materials with the aid of molecular templates—a way towards artificial antibodies. *Angew. Chem. Int. Edn Engl.* **34**, 1812–1832 (1995).
6. Katz, A. & Davis, M. Investigations into the mechanisms of molecular recognition with imprinted polymers. *Macromolecules* **32**, 4113–4121 (1999).
7. Sellergren, B. & Shea, K. J. Influence of polymer morphology on the ability of imprinted network polymers to resolve enantiomers. *J. Chromatogr.* **635**, 39–41 (1993).
8. Vlatakis, G., Anderson, L. I., Müller, R. & Mosbach, K. Drug assay using antibody mimics made by molecular imprinting. *Nature* **361**, 645–647 (1993).
9. Lehn, J.-M. & Eliseev, A. V. Dynamic combinatorial chemistry. *Science* **291**, 2331–2332 (2001).
10. Cousins, G. R. L., Poulsen, S.-A. & Sanders, J. K. M. Molecular evolution: dynamic combinatorial libraries, autocatalytic networks and the quest for molecular function. *Curr. Opin. Chem. Biol.* **4**, 270–279 (2000).
11. Klekota, B. & Miller, B. L. Dynamic diversity and small-molecule evolution: a new paradigm for ligand identification. *Trends Biotechnol.* **17**, 205–209 (1999).
12. Wendland, M. S. & Zimmerman, S. C. Synthesis of cored dendrimers. *J. Am. Chem. Soc.* **121**, 1389–1390 (1999).
13. Schultz, L. G., Zhao, Y. & Zimmerman, S. C. Synthesis of cored dendrimers with internal cross-links. *Angew. Chem. Int. Edn Engl.* **40**, 1962–1966 (2001).
14. Newkome, G. R., Moorefield, C. N. & Vögtle, F. *Dendrimers and Dendrons: Concepts, Syntheses, Perspectives* (Wiley-VCH, Weinheim, 2001).
15. Sanders, J. K. M. Templated chemistry of porphyrin oligomers. *Compreh. Supramolec. Chem.* **9**, 131–164 (1996).
16. Rakon, N. A. & Suslick, K. S. A colorimetric sensor array for odour visualization. *Nature* **406**, 710–714 (2000).
17. Matsui, J., Higashi, M. & Takeuchi, T. Molecularly imprinted polymer as 9-ethyladenine receptor having a porphyrin-based recognition center. *J. Am. Chem. Soc.* **122**, 5218–5219 (2000).
18. Ogoshi, H. & Mizutani, T. Novel approaches to molecular recognition using porphyrins. *Curr. Opin. Chem. Biol.* **3**, 736–739 (1999).
19. Bhyrappa, P., Young, J. K., Moore, J. S. & Suslick, K. S. Dendrimer-metalloporphyrins: synthesis and catalysis. *J. Am. Chem. Soc.* **118**, 5708–5711 (1996).
20. Dandliker, P. J., Diederich, F., Gisselbrecht, J.-P., Louati, A. & Gross, M. Water-soluble dendritic iron porphyrins: synthetic models of globular heme proteins. *Angew. Chem. Int. Edn Engl.* **34**, 2725–2728 (1996).
21. Sadamoto, R., Tomioka, N. & Aida, T. Photoinduced electron transfer reactions through dendrimer architecture. *J. Am. Chem. Soc.* **118**, 3978–3979 (1996).
22. Balzani, V. *et al.* Dendrimers based on photoactive metal complexes. Recent advances. *Coord. Chem. Rev.* **219–221**, 545–572 (2001).
23. Hawker, C. J. & Frechet, J. M. J. A new convergent approach to monodisperse dendritic macromolecules. *J. Am. Chem. Soc.* **112**, 7638–7647 (1990).
24. Trnka, T. M. & Grubbs, R. H. The development of L₂X₂Ru = CHR olefin metathesis catalysts: an organometallic success story. *Acc. Chem. Res.* **34**, 18–29 (2001).
25. Coates, G. W. & Grubbs, R. H. Quantitative ring-closing metathesis of polyolefins. *J. Am. Chem. Soc.* **118**, 229–230 (1996).
26. Adler, A. D. *et al.* A simplified synthesis of meso-tetraphenylporphyrin. *J. Org. Chem.* **32**, 476 (1967).
27. Rho, T. & Abuh, F. One-pot synthesis of pyrimidine-5-carboxaldehyde and ethyl pyrimidine-5-carboxylate by utilizing pyrimidin-5-yl-lithium. *Synth. Commun.* **24**, 253–256 (1994).
28. Collman, J. P. *et al.* Oxygen binding to cobalt porphyrins. *J. Am. Chem. Soc.* **100**, 2761–2766 (1978).

Supplementary Information accompanies the paper on Nature's website (<http://www.nature.com/nature>).

Acknowledgements

We thank W.A. Goddard and T. Cagin for help with dendrimer modelling. This work was funded by the NIH and the US Army Research Office. I.Z. thanks the Arnold and Mabel Beckman Foundation for a Beckman fellowship.

Competing interests statement

The authors declare that they have no competing financial interests.

Correspondence and requests for materials should be addressed to S.C.Z. (e-mail: sczimmer@uiuc.edu).

Tungsten isotope evidence from ~3.8-Gyr metamorphosed sediments for early meteorite bombardment of the Earth

Ronny Schoenberg*, **Balz S. Kamber***, **Kenneth D. Collerson*** & **Stephen Moorbath†**

* *Advanced Centre for Queensland University Research Excellence (ACQUIRE), The University of Queensland, St Lucia, Queensland 4072, Australia*
 † *Department of Earth Sciences, University of Oxford, Parks Road, Oxford OX1 3PR, UK*

The 'Late Heavy Bombardment' was a phase in the impact history of the Moon that occurred 3.8–4.0 Gyr ago, when the lunar basins with known dates were formed^{1,2}. But no record of this event has yet been reported from the few surviving rocks of this age on the Earth. Here we report tungsten isotope anomalies, based on the ¹⁸²Hf–¹⁸²W system (half-life of 9 Myr), in metamorphosed sedimentary rocks from the 3.7–3.8-Gyr-old Isua greenstone belt of West Greenland and closely related rocks from northern Labrador, Canada. As it is difficult to conceive of a mechanism by which tungsten isotope heterogeneities could have been preserved in the Earth's dynamic crust–mantle environment from a time when short-lived ¹⁸²Hf was still present, we conclude that the metamorphosed sediments contain a component derived from meteorites.

It is widely conjectured that the Earth suffered contemporaneous Late Heavy Bombardment (LHB) with the Moon, scaled up proportionally to its much greater gravitational cross-section. Earth's estimated³ mass accretion rate during the LHB was of the order of (1–2) × 10¹⁵ g yr⁻¹, or (2–4) × 10⁻⁴ g cm⁻². Over a 100-Myr period of LHB, this accretion rate would have yielded (1–2) × 10²³ g of material. If added as a continuous veneer over the entire planet, this would correspond to 200 t m⁻². The distinct deuterium/hydrogen ratio of the terrestrial hydrosphere⁴ argues against significant cometary accretion, whereas compositions of projectiles in lunar impact melts⁵ indicate infall from asteroids of enstatite chondrite or iron meteorite parentage. Thus, unless the Earth's early crust was continually recycled into the mantle, it should be possible to detect chemical 'fingerprints' of the LHB in the oldest terrestrial sediments.

In a recent study⁶, the extinct radioactive decay scheme ⁵³Mn–⁵³Cr (half-life, 3.7 Myr) was used to detect meteoritic infall in Cretaceous/Tertiary (K/T) boundary sediments. As Cr isotopes in all classes of meteorites and terrestrial samples are distinct, discovery of a non-terrestrial Cr isotope composition⁶ confirmed extraterrestrial origin. A similar opportunity for detecting meteoritic infall is afforded by the ¹⁸²Hf–¹⁸²W system (half-life, 9 Myr). By analogy with the homogeneous terrestrial Cr isotope composition⁶, any variations in W isotope composition that may have existed in the first ~60 Myr of Earth's history would have been homogenized by convection in the early mantle. Therefore the terrestrial W isotope composition is constant^{7,8}. Indeed, all our terrestrial samples other than the early Archaean metamorphosed sediments (metasediments) yield a constant ¹⁸²W/¹⁸³W ratio (Fig. 1 and Table 1) of 0.10 ± 0.22 ε_W units (where ε_W is the deviation, in 0.1‰, from the terrestrial ¹⁸²W/¹⁸³W ratio), identical to our standard (ACQUIRE-W), which was reproduced at 0.00 ± 0.10 ε_W.

In contrast, a well-resolved W isotope variability exists among different classes of meteorites. Iron meteorites⁹ have much lower ¹⁸²W/¹⁸³W ratios (Fig. 1) of, on average, -3.7 ε_W, reflecting removal of metal-loving W from silicate into the core of planete-

simals when most ^{182}W was still present. Enstatite chondrites¹⁰ yield ϵ_{W} of -2.2 , and differentiated basaltic meteorites, such as eucrites, contain radiogenic W (ref. 11) with ϵ_{W} up to $+39$. Although less reproducible, ordinary chondrites^{12,13} also show resolvably less radiogenic W from -2.0 to $-0.64 \epsilon_{\text{W}}$ compared to the accessible Earth. There is disagreement about the W isotope composition of carbonaceous chondrites, but the most recent determinations^{7,13} in the carbonaceous chondrite Allende yielded -2.2 and $-2.0 \epsilon_{\text{W}}$. Thus it appears that all classes of meteorites have W isotope compositions different from terrestrial samples, and deviations from the terrestrial W isotope composition necessarily imply extraterrestrial W.

The six 3.7–3.8-Gyr amphibolite-facies metasediments from Greenland and northern Labrador studied here belong to the Isua greenstone belt (IGB)¹⁴ and to the Nulliak supracrustal sequence¹⁵, respectively, and were probably deposited during the waning phase of the LHB. The sedimentary precursors of the samples are interpreted as erosion products of mainly mafic rocks (see Supplementary Information). Four of the six early Archaean metasediment samples have resolvably less radiogenic W than the accessible Earth, with ϵ_{W} values ranging from -0.44 to -1.23 (Table 1, Fig. 1). All four data points were replicated on separate aliquots (6X, 4X, 2X, 2X). One sample (KC/91/55c), with large anomaly ($-1.09 \pm 1.04 \epsilon_{\text{W}}$) but also large uncertainty, was not replicated owing to insufficient W yield. Tungsten in a further sample is indistinguishable from the terrestrial average ($+0.07 \pm 0.46 \epsilon_{\text{W}}$). Importantly, because the stable isotope ratios ($^{183}\text{W}/^{186}\text{W}$ and

$^{184}\text{W}/^{186}\text{W}$) of all samples were exactly reproduced to the ACQUIRE standard values (see Supplementary Information), these ^{182}W anomalies are real, and cannot be attributed to spectral interference on a stable W isotope used for mass bias correction. As shown previously¹², the existence of a W isotope anomaly can be corroborated by study of the stable isotope ratio data. To our knowledge, these are the first terrestrial samples shown to contain W isotope anomalies.

Two observations are of particular importance for interpreting this W isotope array. First, an early Archaean terrestrial W crustal average sample (prepared by homogenizing equal aliquots of 24 samples of ~ 3.8 -Gyr igneous felsic and mafic gneisses¹⁶) yields the terrestrial W isotope ratio ($-0.12 \epsilon_{\text{W}}$; Table 1), implying that unradiogenic W was not characteristic of the early Archaean silicate Earth. Hence the most plausible explanation for the unradiogenic W isotope compositions is that a proportion of the W in the metasediments is of extraterrestrial origin. Second, there is strong curved covariation between W isotope composition and several trace element ratios in the sample suite (Fig. 2). The highest correlation coefficients are obtained for logarithmic fits between W isotope compositions and Cr/Ti (Fig. 2) and Ni/Nb ratios. This implies that unradiogenic W was introduced from an erosion source rich in compatible elements. Both chondrites and iron meteorites are rich in Ni and Cr, and have unradiogenic W. Indeed, the logarithmic fit through the metasediment data (Fig. 2a) extrapolates to chondrite and iron meteorite data points.

This does not mean that the metasediments are impact ejecta composed of mixed terrestrial and meteoritic debris. It is more plausible that when these rocks were deposited as water-lain sediments they were fed from weathered terrestrial rock from the eroding land surface, and from meteorite debris that had collected on that surface during the LHB, because the metasediment data do

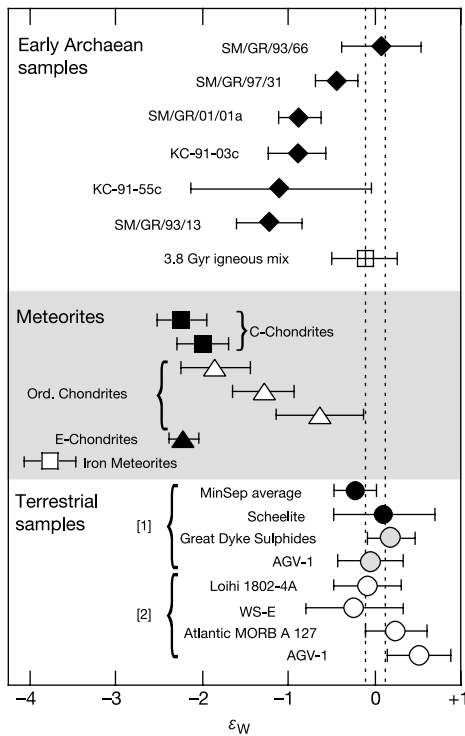


Figure 1 Values of ϵ_{W} for terrestrial rocks, meteorites and early Archaean samples relative to the composition of a tungsten standard, ACQUIRE-W. Dashed lines show 2 s.d. of mean uncertainty envelope of the standard ($n = 46$). Grey circles, terrestrial samples measured previously⁷; filled circles, present results (Table 1). Results highlighted with [1] were analysed at the University of Queensland. Open circles, previously published^{8,21} terrestrial samples. Results highlighted with [2] were analysed at the University of Michigan. Open square, average of published iron meteorites⁹; filled triangle, average of bulk rock enstatite chondrites¹⁰; open triangles, bulk rock ordinary chondrites¹²; filled squares, new data for Allende carbonaceous chondrite^{7,13}. Crossed square, average early Archaean crust (text and Table 1); filled diamonds, early Archaean metasediments (text and Table 1). External error (22 p.p.m.) was assigned to samples with smaller internal errors.

Table 1 Tungsten isotope data

Sample	$^{182}\text{W}/^{183}\text{W}$	\pm	ϵ_{W}	\pm
Terrestrial samples				
Mean ACQUIRE-W	1.852512	19	+0.00	0.10
Scheelite A	1.852450	15	-0.33	0.08
Scheelite B	1.852545	22	+0.18	0.12
Scheelite C	1.852571	19	+0.32	0.10
Scheelite D	1.852556	33	+0.24	0.18
Average	1.852531	109	+0.10	0.59
MinSep average	1.852470	22	-0.22	0.12
Early Archaean samples—Greenland				
3.8 Gyr igneous mix	1.852490	70	-0.12	0.38
SM/GR/93/13 A	1.852258	89	-1.37	0.48
SM/GR/93/13 B	1.852281	93	-1.25	0.50
SM/GR/93/13 C	1.852308	33	-1.10	0.18
SM/GR/93/13 D	1.852306	30	-1.11	0.16
SM/GR/93/13 E	1.852230	33	-1.52	0.18
SM/GR/93/13 F	1.852325	37	-1.01	0.20
Average	1.852284	71	-1.23	0.38
SM/GR/01/01a A	1.852339	122	-0.93	0.66
SM/GR/01/01a B	1.852356	44	-0.84	0.24
Average	1.852348	24	-0.89	0.13
SM/GR/97/31 A	1.852427	104	-0.45	0.56
SM/GR/97/31 B	1.852431	63	-0.43	0.34
Average	1.852429	6	-0.44	0.03
SM/GR/93/66	1.852525	85	+0.07	0.46
Early Archaean samples—Labrador				
KC-91-55c	1.852309	193	-1.09	1.04
KC-91-03c A	1.852355	41	-0.85	0.22
KC-91-03c B	1.852343	74	-0.91	0.40
KC-91-03c C	1.852304	30	-1.12	0.16
KC-91-03c D	1.852379	26	-0.72	0.14
Average	1.852345	62	-0.90	0.34

All measurements were obtained using our previously outlined procedure⁷, except that samples were treated with aqua regia before W purification. Replicate analysis represent separately digested aliquots. All uncertainties are given at 95% confidence. Samples: ACQUIRE-W standard prepared from a high purity W ribbon ($n = 46$); Scheelite is a museum specimen from the late Archaean eastern Yilgarn craton, Australia; MinSep average contains surplus mineral separates from metamorphic and igneous rocks ranging from 0.4 to 3.8 Gyr; 3.8-Gyr igneous mix consists of equal aliquots of 17 felsic and 7 mafic ~ 3.8 -Gyr gneisses from south of the IGB¹⁶.

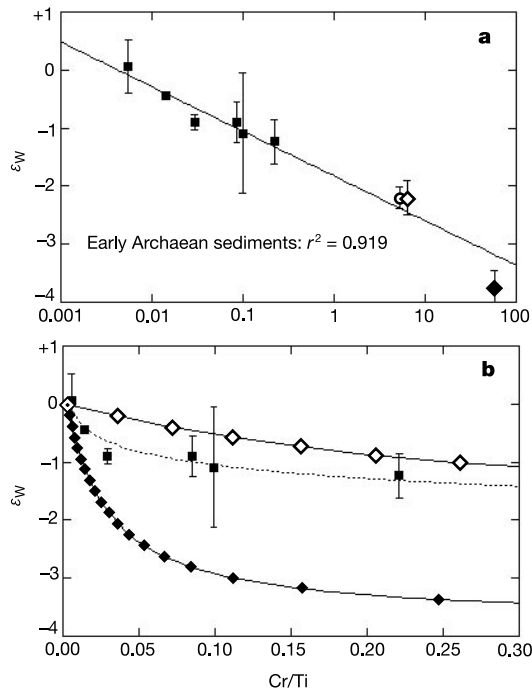


Figure 2 Comparison of ϵ_W to Cr/Ti ratio. **a**, Covariation between ϵ_W and Cr/Ti ratio (note that the x axis is on a logarithmic scale). All metasediment data points from this study (filled squares) define a tight ($r^2 = 0.919$) logarithmic fit (solid line). The fit extends to average enstatite chondrites¹⁰ (open circle), the carbonaceous chondrite Allende^{7,13} (open diamond), and close to average iron meteorite⁹ (solid diamond). Elemental abundance data from refs 17 and 22. Iron meteorites were assigned a Ti abundance of 2 p.p.m., based on the observation¹⁷ that troilite inclusions contain about 10 p.p.m. Ti. **b**, Comparison of metasediment data (solid squares with error bars connected by dashed line representing logarithmic fit) with model mixing hyperbolae. One hyperbola (open diamonds) was calculated between a hypothetical chondrite endmember (data sources as in **a**) and a terrestrial endmember using Cr and Ti concentration data from the IGB metapelite with the lowest known Cr/Ti ratio (0.002) and the lowest observed W content of 100 p.p.b. This endmember represents the Hadean crust, and was assigned an ϵ_W of zero. The second hyperbola (filled diamonds) was calculated between a hypothetical iron meteorite endmember (data sources as in **a**) and the terrestrial endmember. In this case, the terrestrial endmember was assigned a relatively high W content of 3,000 p.p.b.

not show the appropriate hyperbolic relationship (Fig. 2b) predicted by mixing of unmodified terrestrial and meteorite debris. We propose that weathering of meteoritic debris caused preferential liberation of certain elements, depending on the stability of the host minerals in the Hadean atmosphere and hydrosphere. For example, most Cr in iron-meteorite is hosted by troilite (FeS), whereas all W is found in the FeNi metal phase¹⁷. Although W isotopes cannot be used to directly identify the nature of the meteoritic impactors, our data nevertheless provide evidence for the oldest impact event(s) so far discovered on Earth, lending support to interpretation of slightly increased Ir concentrations in some IGB lithologies¹⁸.

Most of the studied metasediments contain particles of carbon. In particular, sample SM/GR/01/01a is from the same outcrop where Rosing¹⁹ described discrete graphite microparticles with isotopically light C ($\delta^{13}\text{C}$ approximately -19‰), which he interpreted as biogenic. However, in view of the present evidence for extraterrestrial W in this sample, the possibility needs to be considered that the graphite represents insoluble carbon particles from carbonaceous chondrites, with $\delta^{13}\text{C}$ of about -18‰ (ref. 20). □

Received 26 March; accepted 18 June 2002; doi:10.1038/nature00923.

1. Ryder, G. Lunar samples, lunar accretion and the early bombardment of the Moon. *Eos* 71, 322–323 (1990).
2. Cohen, B. A., Swindle, T. D. & King, D. A. Support for the lunar cataclysm hypothesis from lunar

meteorite impact melt ages. *Science* 290, 1754–1756 (2000).

3. Anbar, A. D., Zahnle, K. J., Arnold, G. L. & Mojzsis, S. J. Extraterrestrial iridium, sediment accumulation and the habitability of the early Earth's surface. *J. Geophys. Res.* 106, 3219–3236 (2001).
4. Meier, R. & Owen, T. C. Cometary deuterium. *Space Sci. Rev.* 90, 33–43 (1999).
5. Kring, D. A. & Cohen, B. A. Cataclysmic bombardment throughout the inner solar system 3.9–4.0 Ga. *J. Geophys. Res.* E 107(2), 4-1–4-5 (2002).
6. Shukolyukov, A. & Lugmair, G. W. Isotopic evidence for the Cretaceous-Tertiary impactor and its type. *Science* 282, 927–929 (1998).
7. Schoenberg, R., Kamber, B. S., Collerson, K. D. & Eugster, O. New W-isotope evidence for rapid terrestrial accretion and very early core formation. *Geochim. Cosmochim. Acta* (in the press).
8. Lee, D. C. & Halliday, A. N. Hf-W isotopic evidence for rapid accretion and differentiation in the early solar system. *Science* 274, 1876–1879 (1996).
9. Horan, M. F., Smoliar, M. I. & Walker, R. J. ¹⁸²W and ¹⁸⁷Re-¹⁸⁷Os systematics of iron meteorites: Chronology for melting, differentiation, and crystallization in asteroids. *Geochim. Cosmochim. Acta* 62, 545–554 (1998).
10. Lee, D. C. & Halliday, A. N. Accretion of primitive planetesimals: Hf-W isotopic evidence from enstatite chondrites. *Science* 288, 1629–1631 (2000).
11. Quitté, G., Birck, J. L. & Allègre, C. J. ¹⁸²Hf-¹⁸²W systematics in eucrites: the puzzle of iron segregation in the early solar system. *Earth Planet. Sci. Lett.* 184, 83–94 (2000).
12. Lee, D. C. & Halliday, A. N. Hf-W internal isochrons for ordinary chondrites and the initial ¹⁸²Hf/¹⁸⁰Hf of the solar system. *Chem. Geol.* 169, 35–43 (2000).
13. Yin, Q.-Z. *et al.* New Hf-W data that are consistent with Mn-Cr chronology: implications for early solar system evolution. *Lunar Planet. Sci.* XXXIII, A1700 (2002).
14. Appel, P. W. U. & Moorbath, S. Exploring earth's oldest geological record in Greenland. *Eos* 80, 257–264 (1999).
15. Nutman, A. P. & Collerson, K. D. Very early Archaean crustal-accretion complexes preserved in the North Atlantic craton. *Geology* 19, 791–794 (1991).
16. Nutman, A. P., Bennett, V. C., Friend, C. R. L. & Norman, M. D. Meta-igneous (non-gneissic) tonalites and quartz-diorites from an extensive ca. 3800 Ma terrain south of the Isua supracrustal belt, southern West Greenland: constraints on early crust formation. *Contrib. Mineral. Petrol.* 137, 364–388 (1999).
17. Mason, B. *Handbook of Elemental Abundances in Meteorites* (Gordon and Breach Science, New York, 1971).
18. Koeberl, C., Reimold, W. U., McDonald, I. & Rosing, M. T. in *Impacts and the Early Earth* (eds Gilmour, I. & Koeberl, C.) 73–97 (Springer, Heidelberg, 1999).
19. Rosing, M. T. ¹³C-depleted carbon microparticles in >3700-Ma sea-floor sedimentary rocks from west Greenland. *Science* 283, 674–676 (1999).
20. Kerridge, J. F. Carbon, hydrogen and nitrogen in carbonaceous chondrites: Abundances and isotopic compositions in bulk samples. *Geochim. Cosmochim. Acta* 49, 1707–1714 (1985).
21. Lee, D. C., Halliday, A. N., Snyder, G. A. & Taylor, L. A. Age and origin of the moon. *Science* 278, 1098–1103 (1997).
22. Wasson, J. T. & Kallemeyn, G. W. Compositions of chondrites. *Phil. Trans. R. Soc. Lond. A* 325, 535–544 (1988).

Supplementary Information accompanies the paper on Nature's website (<http://www.nature.com/nature>).

Acknowledgements

We thank T. Ewart for discussion and G.W. Lugmair for his review. S.M. collected the Greenland samples under the auspices of the Isua Multidisciplinary Project, and thanks P.W.U. Appel for logistic support. R.S. and B.S.K. thank P. Greenfield for financial support. Analytical costs were partly covered by a UQ New Staff start-up grant to R.S. Collection of the Northern Labrador samples by K.D.C. was financially supported by NSF.

Competing interests statement

The authors declare that they have no competing financial interests.

Correspondence and requests for materials should be addressed to R.S. (e-mail: ronny@earthl.uq.edu.au).

A long-tailed, seed-eating bird from the Early Cretaceous of China

Zhonghe Zhou & Fucheng Zhang

Institute of Vertebrate Paleontology and Paleoanthropology, Chinese Academy of Sciences, PO Box 643, Beijing 100044, China

The lacustrine deposits of the Yixian and Jiufotang Formations in the Early Cretaceous Jehol Group in the western Liaoning area of northeast China are well known for preserving feathered dinosaurs, primitive birds and mammals^{1–3}. Here we report a large basal bird, *Jeholornis prima* gen. et sp. nov., from the Jiufotang